



Research paper

Effect of particle size and charge on the network properties of microsphere-based hydrogels

Sophie R. Van Tomme^{a,*}, Cornelus F. van Nostrum^a, Marjolein Dijkstra^b, Stefaan C. De Smedt^c, Wim E. Hennink^a

^a Department of Pharmaceutics, Utrecht University, Utrecht, The Netherlands

^b Department of Physics and Astronomy, Utrecht University, Utrecht, The Netherlands

^c Department of Pharmaceutics, Ghent University, Ghent, Belgium

ARTICLE INFO

Article history:

Received 5 December 2007

Accepted in revised form 28 May 2008

Available online 6 June 2008

Keywords:

Particle size distribution

Zeta potential

Dextran microspheres

Hydrogels

Network properties

Injectability

Computer simulations

ABSTRACT

This work describes the tailorability of the network properties of self-assembling hydrogels, based on ionic crosslinking between dextran microspheres. Copolymerization of hydroxyethyl methacrylate-derivatized dextran (dex-HEMA), emulsified in an aqueous poly(ethylene glycol) (PEG) solution, with methacrylic acid (MAA) or dimethylaminoethyl methacrylate (DMAEMA) resulted in negatively or positively charged microspheres, respectively, at physiological pH. The monomer/HEMA ratio ranged between 6 and 57, resulting in microspheres with zeta (ζ)-potentials from -6 to -34 mV and $+3$ to $+23$ mV, for the monomers MAA and DMAEMA, respectively. By altering the emulsification procedure, microsphere batches with various sizes and size distributions were obtained. The aim of the research was to assess the effect of particle size (distribution) and charge on the network properties of the macroscopic hydrogels. The ability to tailor the mechanical properties such as strength and elasticity increases the potential of the hydrogels to be used in a variety of pharmaceutical applications. Additionally, the injectability of these self-assembling hydrogels was investigated. Injectability is an important feature of drug delivery systems, since it allows avoiding surgery. Rheological analysis showed that an increasing surface charge of the microspheres led to stronger hydrogels. Relatively small microspheres ($7\ \mu\text{m}$) with a narrow size distribution (99% smaller than $14\ \mu\text{m}$) gave rise to stronger hydrogels when compared to larger microspheres of $20\ \mu\text{m}$ with a broad distribution (99% smaller than $50\ \mu\text{m}$). When small microspheres were combined with large microspheres of opposite charge, it was found that the strongest gels were obtained with 75% small and 25% large microspheres, instead of equal amounts (50/50) of positively and negatively charged microspheres. Computer modeling confirmed these findings and showed that the most favorable composition, related to the lowest potential energy, comprised of 75% small microspheres. Taking both charge and size effects into account, the storage moduli (G') of the almost fully elastic hydrogels could be tailored from 400 to 30,000 Pa. Injectability tests showed that hydrogels (G' up to 4000 Pa) composed of equal amounts of oppositely charged microspheres (-7 and $+6$ mV, average particle size $7\ \mu\text{m}$) could be injected through 25G needles using a static load of 15 N, an ISO accepted value. In conclusion, a variety of options to control the network properties of macroscopic hydrogels are provided, related to the charge and particle size of the composing dextran microspheres. Furthermore, it is shown that the hydrogels are injectable, making them attractive candidates for a diversity of pharmaceutical applications.

© 2008 Elsevier B.V. All rights reserved.

1. Introduction

Controlled delivery of pharmaceutically active proteins is an important topic in the advanced drug delivery field. The bioavailability of proteins after oral administration is low due to chemical

and physical degradation in the gastrointestinal (GI) tract. Parenteral delivery avoids the harsh conditions in the GI tract, but is associated with a lower patient comfort due to repeated administration [1]. Numerous approaches have been evaluated to obtain a prolonged circulation time of the protein (e.g. by conjugation to poly(ethylene glycol) (PEG)) [2] and to assure the bioactivity of the therapeutic is preserved. The latter can be accomplished by entrapment of the protein into polymeric matrices. Various delivery vehicles were designed for the controlled release of bioactive proteins covering among others nanoparticles [3–5], microspheres [6–9], and macroscopic hydrogels [10–12]. Special attention

* Corresponding author. Department of Pharmaceutics, Utrecht Institute for Pharmaceutical Sciences (UIPS), Utrecht University, Sorbonnelaan 16, P.O. Box 80082, 3508 TB Utrecht, The Netherlands. Tel.: +31 30 253 7308; fax: +31 30 251 7839.

E-mail address: s.r.vantomme@uu.nl (S.R. Van Tomme).

should be given to the structural changes of the proteins that might be induced during encapsulation in the delivery system [1]. Damage of these fragile molecules and as a result, loss of their therapeutic activity, e.g. as a result of exposure to organic solvent or crosslinking agents, can be avoided when making use of self-assembling systems [13]. *In situ* formation of hydrogels, mainly based on physical crosslinking between polymer chains can be accomplished through, among others, hydrogen bonding [14,15], crystallization [16], hydrophobic interactions as a result of temperature changes [17], ionic interactions [18–20], or stereocomplexes [21,22]. Besides in the protein delivery field, hydrogels have been widely used in tissue engineering applications [23–27]. Hydrogels do not only act as scaffolds, embedding cells and providing support for newly formed tissue, but they can also deliver growth factors and other signaling proteins at the right site in a sustained manner [28].

A variety of natural and synthetic polymers have been used for the design of hydrogel matrices, of which the latter provide more control over chemical and physical properties. Dextran is an attractive polymer for hydrogel formulations, meeting most of the requirements regarding biocompatibility and biodegradability [29]. Recently, we described a novel injectable self-gelling system based on physical crosslinking between dextran-based microspheres, creating macroscopic hydrogels with tailorable network properties [18]. The mobility of model proteins in the charged network as well as their release from the hydrogels has been studied intensively [30]. Furthermore, it was found that the oppositely charged microspheres showed a different degradation behavior, providing various delivery options in case a bioactive substance would be entrapped between as well as inside the individual microspheres [30].

The aim of this paper was to assess the effect of the charge and size of the dextran microspheres on the network properties of the corresponding macroscopic hydrogels. It can be anticipated that a higher particle surface charge will lead to stronger inter-particle interactions and thus more rigid hydrogels. Furthermore, it is very likely that hydrogels prepared with monodisperse particles will possess different features compared to those consisting of particles with a broad size distribution. Investigating the effect of these variables on the network properties of the hydrogels made it possible to fine tune the system, regarding hydrogel strength and elasticity. Lastly, and importantly for applications, the injectability of these hydrogel systems was studied. Especially for protein delivery applications, it is beneficial if surgery can be avoided and if the delivery system can be injected subcutaneously or intramuscularly. For this purpose, the reversibility of the hydrogel formation was evaluated. Previously, it was shown that upon increasing shear stress, these microsphere-based hydrogels started to flow, while upon removal of the stress, the network was reformed [18]. In the current research, the injectability was investigated by means of compression, using syringes equipped with a fixed needle. The displacement of the plunger upon static load was measured and examined for compatibility with ISO standards.

2. Materials and methods

2.1. Materials

Dextran T40 (from *Leuconostoc* ssp.), *N,N,N',N'*-tetramethylethylenediamine (TEMED) and 2-hydroxyethyl methacrylate (HEMA) were obtained from Fluka (Buchs, Switzerland). Poly(ethylene glycol) (PEG) 10000 and potassium peroxodisulfate (KPS) were provided by Merck (Darmstadt, Germany). *N*-2-Hydroxyethylpiperazine-*N'*-2-ethanesulfonic acid (Hepes) was purchased from Acros Chimica (Geel, Belgium). Methacrylic acid (MAA) and *N,N*-di-

methyl aminoethyl methacrylate (DMAEMA) were provided by Sigma–Aldrich (Zwijndrecht, The Netherlands).

2.2. Preparation of charged dex-HEMA microspheres

Dextran was derivatized with hydroxyethyl methacrylate (dex-HEMA) according to van Dijk-Wolthuis et al. [31]. The degree of substitution (DS, i.e. the number of HEMA groups per 100 glucopyranose units) used in this study was 10. Charged dex-HEMA microspheres were prepared in an all-aqueous environment as described previously with some minor modifications [32,33]. Charged monomers, methacrylic acid (MAA) or *N,N*-dimethyl aminoethyl methacrylate (DMAEMA) were added to dex-HEMA prior to emulsification in PEG solution. The monomer/HEMA ratio was varied from 6 to 57, using 12.5–125 mM monomer, respectively. Most batches were prepared on a 50 g scale (total mixture), in 50 ml plastic vials. The emulsion was obtained by vortexing for 3 min, after which KPS and TEMED were added to polymerize the dispersed dextran derivatives. To obtain particles with a relatively narrow particle size distribution, large batches (500 g scale) of negatively and positively charged microspheres (monomer/HEMA ratio of 11) were prepared by means of an Ultra-Turrax (30 min, 11,000 rpm) (IKA®-WERKE GMBH & CO.KG, Staufen, Germany) [18]. The microsphere dispersions were consecutively sieved through a series of metal sieves with decreasing pore size (50, 20, 15, 10 and 5 μm) by means of ultrasonic vibrations (using a wet sieving system that comprises of an Electronic Sieve Vibrator (EMS 755) and an Ultrasonic Processor (UDS 751), purchased from Topaz GmbH, Dresden, Germany). The final dispersions were centrifuged at 4000 rpm for 1 h after which the pellets and supernatants were collected separately. Microspheres (monomer/HEMA ratio of 11) with a relatively larger average particle size and a broad size distribution were obtained by emulsification of the dextran/PEG mixture (on a 75 g scale in a 125 ml beaker) with a 3-blade propeller stirrer at 60 rpm for 1 h prior to polymerization with KPS and TEMED. Finally, for all preparation procedures, after three washing and centrifugation steps with reversed osmosis water, the microspheres were freeze-dried.

Table 1 summarizes all microsphere batches, including preparation method and properties. A sample code (M1–M16) was given to each microsphere type and was used throughout the text to identify specific microsphere batches.

2.3. Characterization of the charged microspheres

2.3.1. Determination of the particle size and particle size distribution

Particle size and particle size distribution of the various microsphere batches were obtained using an Optical Particle Sizer (Accusizer Model 780, Particle Sizing Systems, Santa Barbara, USA). Calibration of the instrument was performed with latex beads (1–100 μm) (Duke Scientific Corporation). The freeze-dried microspheres were suspended in reversed osmosis (r.o.) water prior to the particle size measurement.

Light microscopy images of hydrated microspheres were obtained using a Nikon eclipse TE2000-U (Nikon instruments Europe B.V., Badhoevedorp, The Netherlands).

2.3.2. ζ (zeta)-Potential measurements

The ζ -potential of the microspheres was measured by laser Doppler electrophoresis with a Zetasizer Nano-Z (Malvern Instruments Ltd., Worcestershire, United Kingdom) using a folded capillary cell (DTS 1060). Calibration of the instrument was performed with DTS 1050 latex beads (zeta potential transfer standard, Malvern). The freeze-dried microspheres were suspended in buffer (Hepes 5 mM, pH 7.0, or ammonium acetate 5 mM, pH 6.0) and homogenized thoroughly before the measurement (0.5–1% w/v).

Table 1
Characteristics of the various microsphere (dex-HEMA-MAA and dex-HEMA-DMAEMA) batches

Sample code	MAA/HEMA ratio (mol/mol)	Emulsification method	Vol-wt ^a mean diameter (μm)	99% less than (μm)	ζ-Potential (mV)
<i>Negatively charged microspheres (dex-HEMA-MAA)</i>					
M1	6	Vortex	12	22	−6
M2	11	Vortex	14	28	−8
M3	23	Vortex	11	20	−13
M4	34	Vortex	11	20	−20
M5	45	Vortex	5	12	−27
M6	57	Vortex	9	28	−34
M7	11	Ultraturrax + sieving	7	14	−7
M8	11	Stirrer	16	50	−8
Sample code	DMAEMA/HEMA ratio (mol/mol)	Emulsification method	Vol-wt ^a mean diameter (μm)	99% less than (μm)	ζ-Potential (mV)
<i>Positively charged microspheres (dex-HEMA-DMAEMA)</i>					
M9	6	Vortex	13	29	+3
M10	11	Vortex	13	27	+6
M11	23	Vortex	10	19	+11
M12	34	Vortex	4	15	+16
M13	45	Vortex	4	14	+23
M14	57	Vortex	9	18	+23
M15	11	Ultraturrax + sieving	7	13	+6
M16	11	Stirrer	25	50	+8

The ζ-potentials were measured at pH 7.0 (Hepes buffer, 5 mM). The sample codes were used throughout the manuscript to identify the particular microspheres used for each experiment.

^a Volume-weighted.

2.4. Preparation of microsphere-based hydrogels

Hydrogels were obtained after hydration of freeze-dried positively and negatively charged microspheres. Prior to addition of buffer (Hepes 100 mM, pH 7.0) the positively and negatively charged lyophilized microspheres were intensively mixed. The microspheres were allowed to hydrate for 1 h at 4 °C before rheological analysis of the formed hydrogels was performed. Various weight ratios of positively/negatively charged microspheres were used (specified in the text for each experiment). Unless stated otherwise, the solid content of the gels was 15% (w/w).

2.5. Rheological analysis

Rheological analysis of hydrogels was done using a controlled stress rheometer (AR1000-N, TA Instruments, Etten-Leur, The Netherlands), equipped with an acrylic flat plate geometry (20 mm diameter) and a gap of 500 μm. Hydrogels (200 mg) were prepared as described above and subsequently introduced between the two plates. A solvent trap was used to prevent evaporation of the solvent. The viscoelastic properties of the sample were determined by measuring the G' (shear storage modulus) and G'' (loss modulus) at 20 °C with a constant strain of 1% and constant frequency of 1 Hz. Each experiment was performed thrice, unless stated otherwise.

2.6. Computer modeling of the particle interactions

Computer modeling of the hydrogels was done. It was assumed that the microspheres interact with the Derjaguin–Landau–Verwey–Overbeek (DLVO) screened-Coulomb pair potential $V_{ij}(r)$ [34,35]:

$$\frac{V_{ij}(r)}{k_B T} = Z_i Z_j \lambda_B \frac{e^{\kappa(a_i + a_j)}}{(1 + \kappa a_i)(1 + \kappa a_j)} \frac{e^{-\kappa r}}{r},$$

where r is the distance between two microspheres with respective radii a_i and a_j , and charges $Z_i e$ and $Z_j e$. Here the Bjerrum length is $\lambda_B = e^2 / (4\pi\epsilon\epsilon_0 k_B T)$, with ϵ the relative dielectric constant of the solvent, ϵ_0 the dielectric permittivity of vacuum, e the elementary charge, k_B Boltzmann's constant and T the absolute temperature. The same contact value $\epsilon = |Z_i Z_j| \lambda_B / ((1 + \kappa a_i)(1 + \kappa a_j))$ for all pair interactions was assumed, as the ζ-potentials for the anionic and cationic microspheres are almost equal. The solid fraction was set at 15%

and the ratio of anionic/cationic microspheres was varied. The microspheres were regarded as rigid particles since the pseudo elasticity modulus of the macroscopic hydrogels was up to 100 times smaller than the modulus of the individual microspheres [36]. Furthermore, the negatively charged microspheres were 5 μm in size, while the positively charged ones were 9 μm. Monte-Carlo simulations in the canonical ensemble were performed, i.e. the number of both species, the volume of the box, and the temperature were fixed. A cubic box with linear dimension of 45 μm was used and periodic boundary conditions were applied. For more technical details on the simulations we refer to Frenkel and Smit [37]. Equilibration was checked by monitoring the potential energy of the system U^* , which is the sum of all pair interactions.

$$U^* = \sum_{i=1}^{N-1} \sum_{j=i+1}^N \frac{V_{ij}(r)}{V}.$$

When equilibrium was reached, a production run of 1×10^5 sweeps was performed (one displacement attempt per particle), while sampling was performed once every sweep.

2.7. Injectability of the hydrogels

The injectability of the hydrogels was investigated using a compression device (Lloyd LR5K-plus) fitted with a 100 Newton Load cell (Lloyd Instruments Ltd., Hampshire, United Kingdom). Dispersions or hydrogels (500 mg) were introduced into glass syringes (2 ml, internal diameter = 8.65 ± 0.2 mm) equipped with a fixed needle (25G 5/8 in.), by means of a spatula. The samples were subjected to a static load (5–30 N) for 30 s while the displacement of the plunger was monitored. The syringes were weighted before and after each experiment to measure the amount of sample 'ejected'. The data were processed with Nexygen Ondio software (Lloyd Instruments Ltd.).

3. Results and discussion

3.1. Preparation of dex-HEMA microspheres with various charges and size distributions

Using the water-in-water emulsion preparation procedure, positively and negatively charged dex-HEMA microspheres were ob-

tained by copolymerization with DMAEMA and MAA, respectively, with an equilibrium water content of 70%. The size (distribution) and charge of the microspheres was varied. Table 1 gives an overview of the different batches including sample code and microsphere characteristics.

3.1.1. Effect of the preparation method on the particle size distribution of dex-HEMA-MAA and dex-HEMA-DMAEMA microspheres

Representative size distributions of microspheres obtained via sieving, stirring or vortexing are depicted in Fig. 1.

Emulsification of the dex-HEMA/PEG mixture using a vortex led to polydisperse particles with an average volume-weighted diameter of 10 μm . Ninety-nine percentage of the microspheres were smaller than 20 μm . For three batches prepared by vortexing, a significantly smaller particle size was observed (4–5 μm). To narrow down the particle size distribution, sieving of polydisperse particles was applied. Before sieving, the average particle size was 10 μm . Remarkably, during the sieving process most microspheres were able to pass all sieves, even with the smallest pore size (5 μm). This is possibly due to the high water content of the particles (70%), which makes them quite flexible and allows deformation to penetrate through the pores of the membranes. The final microsphere dispersion was centrifuged, which resulted in a pellet of microspheres with an average size of 7 μm and a relatively narrow size distribution (99% smaller than 13–14 μm) (M7 and M15) (Fig. 2A). Light microscopy images revealed that the supernatant mostly contained fragments of microspheres. The microsphere yield after the sieving and centrifugation steps was $\sim 35\%$. Microspheres with a slightly larger average diameter (16–25 μm) and a broad size distribution (99% smaller than 50 μm) (Fig. 2B) when compared to the particles obtained by vortexing were prepared by creating the dex-HEMA/PEG emulsion at a lower speed with a 3-blade propeller (M8 and M16). A size distribution with two populations was obtained, both smaller than 50 μm (Fig. 1).

3.1.2. Effect of the monomer/HEMA ratio on the ζ -potential of charged dex-HEMA microspheres

Fig. 3 shows that with increasing the monomer/HEMA ratio, the surface charge (reflected by the ζ -potential) of the resulting particles increased. This figure also shows that the ζ -potential (absolute values) of the dex-HEMA-DMAEMA microspheres was slightly lower than the ζ -potential of the dex-HEMA-MAA microspheres prepared at the same monomer/HEMA ratio. Since the pK_a of (p)DMAEMA is between 8.5 and 7.5, depending on the molecular weight of the polymer [38], the DMAEMA units in the network

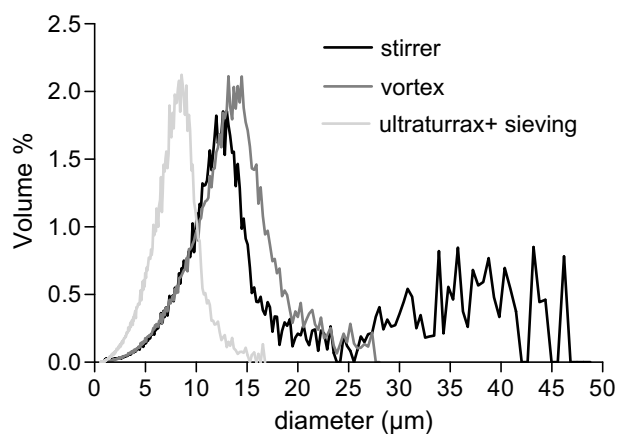


Fig. 1. Particle size distribution (dex-HEMA-MAA microspheres, MAA/HEMA ratio of 11) for different preparation methods (ultraturrax and sieving (M7): light gray line; vortex (M2): gray line; stirrer (M8): black line).

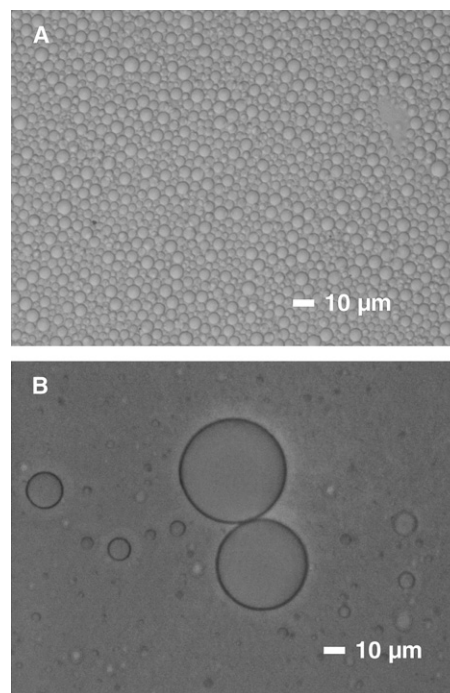


Fig. 2. Light microscopy images of (A) small dex-HEMA-MAA microspheres obtained after sieving of a polydisperse batch (M7), (B) large dex-HEMA-MAA microspheres with a broad-size distribution, prepared at a low speed with a 3-blade propeller (M8).

are not fully protonated at pH 7, while MAA ($pK_a \sim 4.7$ [39]) is fully deprotonated under the same conditions. An alternative explanation is that DMAEMA is less reactive than MAA, leading to less incorporation in the microspheres. Higher ζ -potentials for the DMAEMA particles were found when measuring the particle charge at pH 6 (Fig. 3) confirming the partial protonation at pH 7.0. Dex-HEMA microspheres without additional charged monomer showed a slightly negative ζ -potential (~ -1.3 mV, Fig. 3), likely caused by adsorption of anions.

3.2. Effect of the particle size on the gel strength

Rheology was used to study the effect of the particle size and size distribution on the network properties of microsphere-based

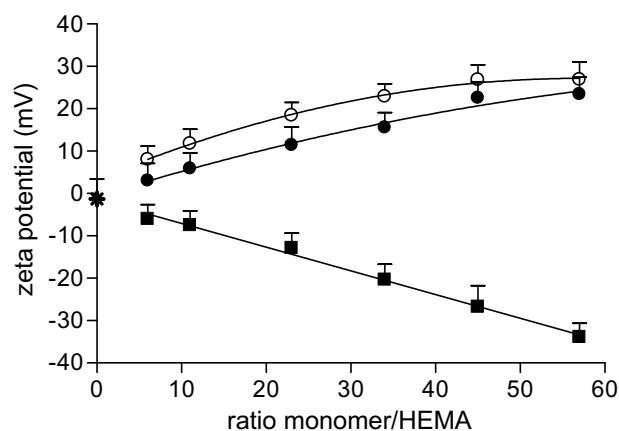


Fig. 3. Effect of the monomer/HEMA ratio on the ζ -potential of dex-HEMA-MAA (■, pH 7) and dex-HEMA-DMAEMA (●, pH 7; ○, pH 6) microspheres (*, dex-HEMA microspheres, pH 7).

hydrogels. It was reported previously that the 1% strain, applied on the hydrogels, was in the linear range [18]. Fig. 4 shows the G' for hydrogels consisting of equal amounts (w/w) of negatively and positively charged microspheres, but with various sizes (small vs. large). The ζ -potential was -7 and -8 mV for dex-HEMA-MAA and $+6$ and $+8$ mV for dex-HEMA-DMAEMA microspheres, while the solid content of the hydrogels was varied (15–25%). When large particles (M8 and M16) were used, no gel formation was observed at a solid content of 15%. At the same concentration of small microspheres (M7 and M15), on the other hand, a hydrogel with a G' of 5000 Pa was formed. A higher percentage solid did lead to gel formation for the large microspheres, but the gels were substantially weaker than those consisting of small particles ($G' = 1100$ and 13,500 Pa, respectively, for 20% solid). A combination of small particles with large particles led to hydrogels with intermediate strength (e.g. $G' = 8300$ Pa for 20% solid).

Various weight ratios of small negatively charged ($7 \mu\text{m}$, -7 mV) and large positively charged ($25 \mu\text{m}$, $+8$ mV) microspheres (M7 and M16) were combined and the gel properties were monitored (15% solid) (Fig. 5). As a comparison, the gel strength (15% solid) was investigated for various weight ratios of negatively and positively charged small microspheres (both $7 \mu\text{m}$, -7 mV and $+6$ mV, respectively) (M7 and M15). As previously shown [18], only negatively charged or positively charged microspheres did not lead to the formation of a gel ($\tan(\delta) > 1$). When a mixture of 80% large positively charged microspheres (M16) and 20% small negatively charged microspheres (M7) was used, no gel formation occurred. The opposite combination, 80% small negatively charged and 20% large positively charged microspheres, led to the formation of an almost fully elastic gel ($G' \sim 1600$ Pa, $\tan(\delta) = 0.1$). Using both small negatively charged microspheres (M7) and small positively charged microspheres (M15), comparable network properties were found for the ratios 20/80 and 80/20 of anionic/cationic microspheres ($G' \sim 2000$ Pa, $\tan(\delta) \sim 0.15$).

For the system described above, the batch of large microspheres (M16) had a high polydispersity (average vol-wt diameter $25 \mu\text{m}$, 99% smaller than $50 \mu\text{m}$) and thus contained a fraction of small particles. Fig. 6 shows the G' of dispersions and hydrogels consisting of microspheres with a less broad size distribution (dex-HEMA-MAA microspheres (M5): $5 \mu\text{m}$, 99% smaller than $12 \mu\text{m}$, -27 mV; dex-HEMA-DMAEMA microspheres (M14): $9 \mu\text{m}$, 99% smaller than $18 \mu\text{m}$, $+23$ mV). No network formation ($\tan(\delta) > 1$) was observed when an excess of large particles was present (75% w/w) and above

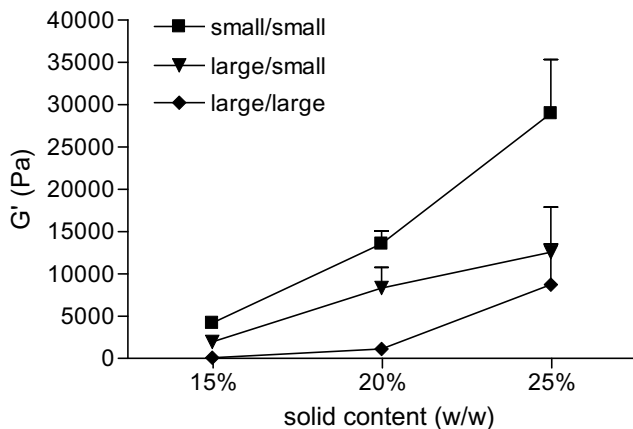


Fig. 4. Storage modulus (G') of hydrogels consisting of equal amounts (w/w) of dex-HEMA-MAA and dex-HEMA-DMAEMA microspheres as a function of the solid content of the hydrogels, for particles with different sizes (small/small (M7 and M15) (■), large/small (M7, M8, M15 and M16) (▼), large/large (M8 and M16) (◆)) ($n = 3$). The $\tan(\delta)$ of the different gels was < 0.1 .

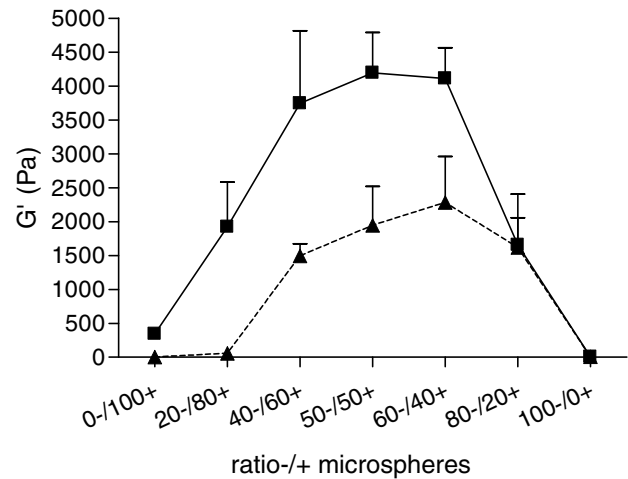


Fig. 5. The effect of the particle size (distribution) of oppositely charged microspheres on the network properties of macroscopic hydrogels, illustrated by the storage modulus (G') of dispersions and hydrogels (15% solid (w/w)) composed of (▲) small negatively charged ($7 \mu\text{m}$, -7 mV) (M7) and large positively charged ($25 \mu\text{m}$, $+8$ mV) (M16) microspheres or (■) only small microspheres (M7 and M15) ($7 \mu\text{m}$, -7 and $+6$ mV) in various ratios (w/w) ($n = 2$).

this concentration gels were formed of which the gel strength (G') increased with increasing fraction of small particles reaching a maximum at 75% small and 25% large microspheres ($G' \sim 19,000$ Pa, $\tan(\delta) \sim 0.06$). At higher percentage of small microspheres, no gel formation was observed. The higher G' values of the hydrogels shown in Fig. 6, compared to those depicted in Fig. 5, can be explained by the higher ζ -potential of the microspheres composing the hydrogels in Fig. 6. In the case described above, the small particles were negatively charged while the large particles were positively charged. The reversed situation was also investigated (dex-HEMA-MAA microspheres (M4): $11 \mu\text{m}$, 99% smaller than $20 \mu\text{m}$, -20 mV; dex-HEMA-DMAEMA microspheres (M12): $4 \mu\text{m}$, 99% smaller than $15 \mu\text{m}$, $+16$ mV). Fig. 6 shows again that a dramatic increase of the gel strength was observed when the amount of small microspheres was increased compared to the fraction of large ones. No hydrogel formation could occur when an

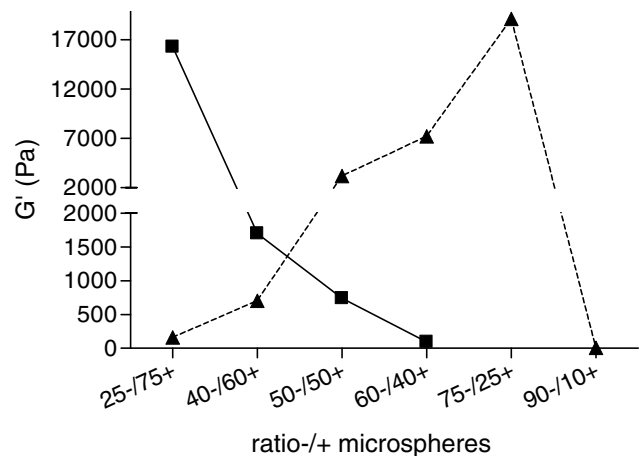


Fig. 6. The effect of the particle size (distribution) of oppositely charged microspheres on the network properties of macroscopic hydrogels, illustrated by the storage modulus (G') of dispersions and hydrogels (15% solid (w/w)) composed of (▲) small negatively charged (M5) ($5 \mu\text{m}$, -27 mV) and large positively charged (M14) ($9 \mu\text{m}$, $+23$ mV) or (■) large negatively charged (M4) ($11 \mu\text{m}$, -20 mV) and small positively charged (M12) ($4 \mu\text{m}$, $+16$ mV) microspheres in various weight ratios.

abundance of large particles was present in the mixture (75%) as evidenced by $\tan(\delta) > 1$.

The results presented in Fig. 6 can be explained by the fact that one large microsphere will be able to interact with many small microspheres. To obtain as many interactions as possible, the number of small microspheres needs to be higher than the number or amount of large microspheres (Fig. 7). For the combination dex-HEMA-MAA microspheres of 5 μm (M5) with dex-HEMA-DMAEMA microspheres of 9 μm (M14) (depicted in Fig. 6), for the ratio where the gel had the highest strength (75–/25+), it can be calculated that the total number of small particles was 17 times higher than the number of large particles. Further, the total area of the small microspheres with an average size of 5 μm was 5 times more than that of the large particles with an average size of 9 μm . It can be anticipated that the large microspheres are able to utilize their surface more efficiently than the small microspheres. Fig. 7 illustrates that the large microspheres can almost use their full surface to interact with the small particles, while the small ones only bind to the large ones at a few connection points.

To fully comprehend the interactions between the negatively and positively charged microspheres of different size, computer modeling was carried out. For various ratios of negative/positive microspheres, the potential energy of the system was calculated. The potential energy is a measure for the strength of the gel and is calculated by summing over all microsphere-interactions. Equally charged microspheres repel, while oppositely charged microspheres attract. The lowest potential energy corresponds to the most favorable composition, i.e. the best stabilized system. Fig. 8 shows the potential energy (U^*) as a function of the ratio of negatively/positively charged microspheres of 5 and 9 μm , respectively. The highest (less negative) U^* was found in those systems with an excess ($\geq 90\%$) of negatively or positively charged particles. As shown in Fig. 6, no gel formation occurs in these cases. The most favorable composition, related to the lowest U^* (most negative) showed to be the system containing $\sim 75\%$ of negatively charged microspheres. Keeping in mind that the anionic microspheres are 'small' (5 μm), compared to the cationic microspheres (9 μm), these findings fully correlate with the rheology data reported in Fig. 6. Strongest gels are obtained when the ratio of small/large particles is 3, as a result of an optimal packing in which the small microspheres fill the pores between the large ones.

3.3. Effect of the microsphere charge on the gel strength

Dex-HEMA-MAA and dex-HEMA-DMAEMA microspheres were prepared with varying monomer/HEMA ratios yielding particles with different ζ -potentials (Fig. 3). Increasing the monomer/HEMA ratio in the initial dextran/PEG mixture from 6 to 23 led to a significant increase in G' of the corresponding hydrogels from 350 to

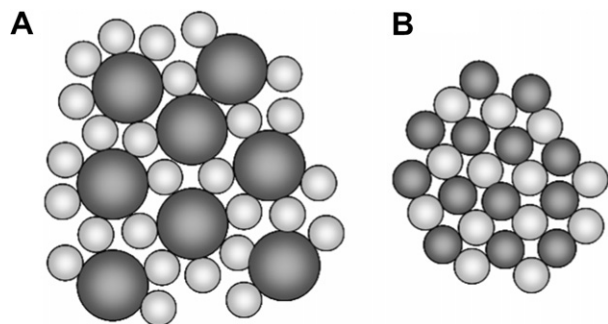


Fig. 7. Schematic presentation of a hydrogel consisting of large and small microspheres (A) and merely small microspheres (B). The dark-colored and light-colored microspheres represent particles of opposite charge.

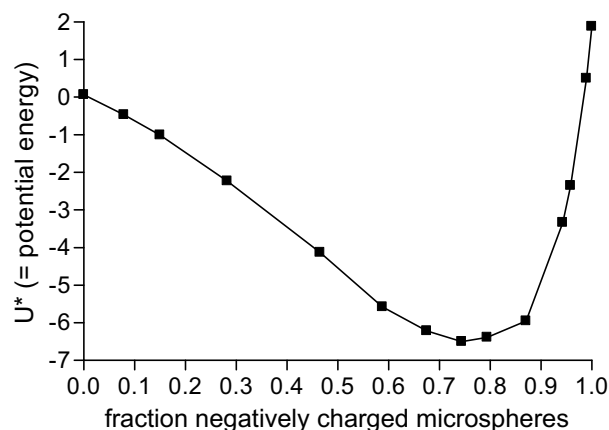


Fig. 8. Calculated potential energy (U^*) as a function of the fraction of negatively charged small microspheres.

6000 Pa (Fig. 9). The $\tan(\delta)$ was in all cases below 0.1, confirming the almost fully elastic properties of the hydrogels. Strikingly, a further increase of the monomer/HEMA ratio led to a decrease of the G' to 1400 Pa. For the highest charge of the particles a slight increase in gel strength to 4000 Pa was again observed.

Table 1 shows that the ζ -potential (absolute value) of the dex-HEMA-DMAEMA microspheres is in most cases less than that of the dex-HEMA-MAA microspheres prepared at the same monomer/HEMA ratio. Therefore, hydrogels were also prepared by combining negatively charged and positively charged microspheres with similar absolute ζ -potentials, instead of with equal monomer/HEMA ratios (data not shown). It was found that the combination of dex-HEMA-MAA microspheres of -6 mV (M1) (average particle diameter 12 μm) with dex-HEMA-DMAEMA microspheres of $+6$ mV (M10) (average particle diameter 13 μm) led to much stronger gels ($G' = 2000$ Pa, $\tan(\delta) = 0.04$) than the combination with dex-HEMA-DMAEMA microspheres of $+3$ mV (M9) (average particle diameter 13 μm) ($G' = 350$ Pa, $\tan(\delta) = 0.08$). Although not as pronounced, this phenomenon was also seen with dex-HEMA-MAA microspheres of -20 mV (M4) (average particle diameter 11 μm) combined with dex-HEMA-DMAEMA microspheres of $+23$ mV (M13) (average particle diameter 4 μm) ($G' = 2250$ Pa, $\tan(\delta) = 0.16$) instead of dex-HEMA-DMAEMA microspheres of $+16$ mV (M12) (average particle diameter 4 μm) ($G' = 1700$ Pa, $\tan(\delta) = 0.13$).

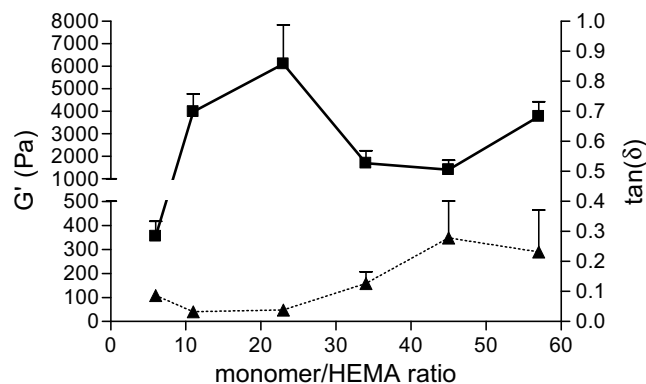


Fig. 9. Storage modulus (G') (\blacksquare) and $\tan(\delta)$ (\blacktriangle) of hydrogels (15% solid) consisting of equal amounts (w/w) of dex-HEMA-MAA and dex-HEMA-DMAEMA microspheres ($n = 3$). The microspheres differed in the monomer/HEMA ratio used for the preparation.

These observations however, do not explain the drop in G' when the monomer/HEMA ratio increased from 23 to 34. As already mentioned, the difference in particle size between the positively and negatively charged microspheres was quite large for the microsphere batches with monomer/HEMA ratios of 34 (M4 and M12) and 45 (M5 and M13), and therefore, as discussed above, the 50/50 weight ratio used is not optimal to obtain the highest gel strength in those cases. Instead of the 50/50 dex-HEMA-MAA/dex-HEMA-DMAEMA microsphere combinations (Fig. 9), the 'optimized' ratios are plotted (Fig. 10). Oppositely charged microspheres were matched according to their ζ -potential, regardless of the microsphere size. Dependent on the size (distribution) different ratios $-/+$ microspheres were required to obtain the highest gel strength. Within each set of combinations, a mixture was considered 'optimized' when the strongest hydrogels were obtained. The characteristics of the various combinations are listed in Table 2. For all combinations, the $\tan(\delta)$ was <0.1 . Compared to Figs. 9 and 10 shows that in line with expectations the G' increased with increasing ζ -potential of the microspheres. Fig. 10 illustrates that, when taking the particle size and ζ -potential into account, hydrogels can be designed with tailorable strength for the aimed application.

3.4. Injectability of the hydrogels

One important application that can be foreseen for the hydrogels composed of oppositely charged dextran microspheres is the use as delivery system for pharmaceutical proteins. Injectability of the delivery systems is preferred, thereby avoiding surgery. The injectability of the microsphere-based hydrogels was evaluated during compression tests in which the hydrogels were loaded

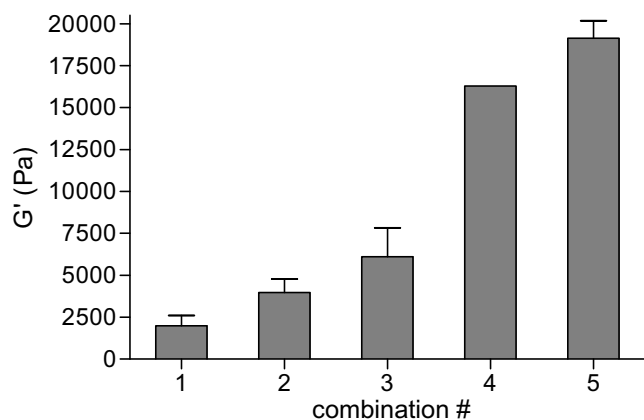


Fig. 10. Storage modulus of hydrogels (15% solid) consisting of various combinations of dex-HEMA-MAA and dex-HEMA-DMAEMA microspheres ($n = 3$, except for No. 4 where $n = 1$). The Combination No. refers to Table 2.

Table 2
Various combinations of dex-HEMA-MAA and dex-HEMA-DMAEMA microspheres and their specific characteristics

Combination No.	Sample code	Monomer/HEMA ratio		ζ -Potential (mV)		Vol-wt mean (μm)		Ratio $-/+$
		-	+	-	+	-	+	
1	M1 and M10	6	11	6	6	12	13	50/50
2	M2 and M10	11	11	8	6	14	13	50/50
3	M3 and M11	23	23	13	11	11	10	50/50
4	M4 and M12	34	34	20	16	11	4	25/75
5	M5 and M14	45	57	27	23	5	9	75/25

into glass syringes (internal diameter = 8.65 ± 0.2 mm), equipped with a fixed 25G (5/8 in.) needle. Such needles are typically used for subcutaneous injection, which is the aimed route of administration for these hydrogel systems. It was shown that the rubber plunger had a low friction (1 N) with the syringe wall.

Next, the injection force required for a dispersion of non-charged dex-HEMA microspheres (15% solid w/w) was studied. A static load of 5 N was applied for 30 s while the displacement of the plunger (= extension) was monitored (Fig. 11A). The dispersion showed to be easily and reproducibly 'ejectable' at a flow of ~ 135 mg/min, under these conditions, as expected.

The behavior of hydrogels (15% solid w/w) composed of equal amounts of small (7 μm) dex-HEMA-MAA (M7) and dex-HEMA-DMAEMA (M15) microspheres, with a monomer/HEMA ratio of 11, corresponding to ζ -potentials of -7 and $+6$ mV, respectively, was investigated at a static load of 30 N. These hydrogels possess a G' of 4000 Pa (Fig. 4). Fig. 11B shows that approximately 15 N was needed to obtain a constant flow, which is regarded acceptable [40]. Compared to the dex-HEMA microsphere-dispersion, the flow rate was smaller, ~ 70 mg/min, for a higher static load (15 N vs. 5 N for dex-HEMA microspheres).

It was shown in Fig. 9 that stronger hydrogels were obtained when the monomer/HEMA ratio of the microspheres was increased from 11 to 23. Fig. 12 shows the differences in displacement of the plunger during three consecutive measurements for hydrogels composed of microspheres with a monomer/HEMA ratio of 11 (M7 and M15) (A) and a monomer/HEMA ratio of 23 (M3 and M11) (B). The latter hydrogels correspond to microspheres with ζ -potentials of -13 and $+11$ mV, particle sizes of 11 and 10 μm and a G' of 6100 Pa (Fig. 9). A static load of 15 N was enough to introduce flow in the systems independent of the microsphere charge, but the injectability of the hydrogels composed of particles with the highest charge ($-13/+11$ mV compared to $-7/+6$ mV) was hampered as evidenced by the decrease in flow speed from ~ 60 mg/min to ~ 10 mg/min during three consecutive experiments. A difference in flow behavior was observed between the

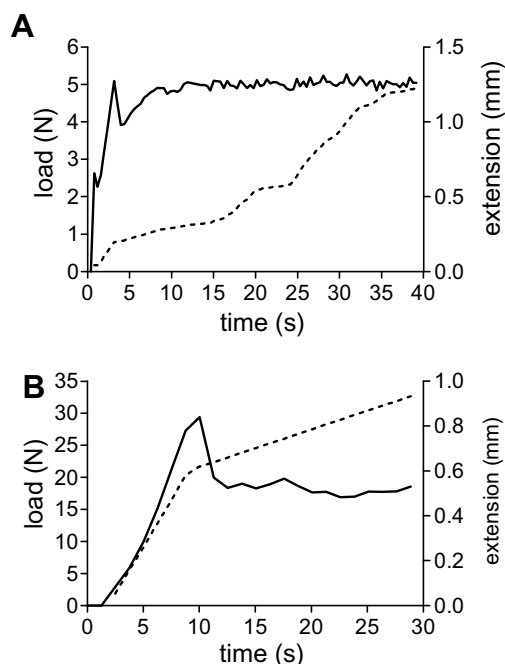


Fig. 11. Extension (---) of (A) a dex-HEMA microsphere-dispersion (15% solid (w/w)) and (B) a hydrogel composed of dex-HEMA-MAA (M7) and dex-HEMA-DMAEMA microspheres (M15) (15% solid (w/w), monomer/HEMA ratio 11) during an injectability test (static load (—)).

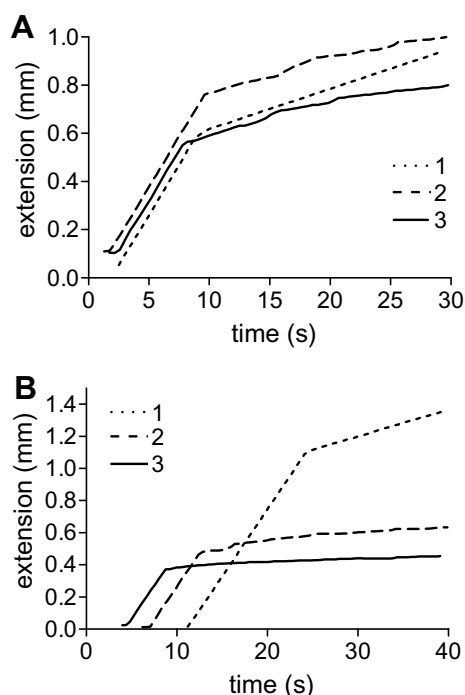


Fig. 12. Displacement of the plunger (extension) during three consecutive compression tests of (A) dex-HEMA-MAA/dex-HEMA-DMAEMA hydrogel (M7 and M15) (monomer/HEMA ratio 11, 15% solid (w/w)) and (B) dex-HEMA-MAA/dex-HEMA-DMAEMA hydrogel (M3 and M11) (monomer/HEMA ratio 23, 15% solid (w/w)).

two differently charged hydrogels. While the hydrogels with particle ζ -potentials of ~ 6 – 7 mV (absolute value) showed the formation of homogenous gel-threads during ejection, the hydrogel with microspheres with a higher ζ -potential (~ 11 – 13 mV, absolute value) was ejected as a discontinuous fiber with water droplets daggling along. The injectability of hydrogels composed of microspheres with an even higher ζ -potential (~ 23 – 27 mV, absolute value), corresponding to monomer/HEMA ratios of 45 (M5 and M13), was not possible under the tested conditions. Initially, water was pushed out of the hydrogel, leading to a denser packing of the microspheres inside the syringe. Eventually, a cake of microspheres remained. Apparently, a higher charge density on the microspheres results in expulsion of water from the hydrogel upon compression and can be explained by the increased inter-particle interactions. These experiments show that it is possible to administer hydrogels (G' up to 4000 Pa), based on dex-HEMA-MAA and dex-HEMA-DMAEMA microspheres (on average 7–10 μm in diameter), using needles suitable for subcutaneous injection, provided that the particle interactions are not too strong. In these particular systems, this corresponds to particle charges typically in the range of 7 mV (absolute value).

4. Conclusions

In this work, the network properties of self-assembling hydrogels based on ionic interactions between dextran microspheres were investigated. Dextran hydrogels have shown to possess favorable properties such as biocompatibility and biodegradability [41]. The potential of the hydrogels described in this paper as protein delivery matrices has been studied previously [42]. In this study a number of options to control their network properties are provided. Both the surface charge of the microspheres and their size and size distribution were varied by adjusting the charged monomer/HEMA ratio and several parameters in the microsphere preparation process. The gel strength showed to be tailorable from 400

to 30,000 Pa, making them suitable for a range of drug delivery and tissue engineering applications in which diverse mechanical properties are required. Hydrogels with a G' up to 4000 Pa showed to be injectable using a force of 15 N, which is accepted by ISO standards.

Acknowledgements

Jan Rikken and Jean-Paul Kleeven from N.V. Organon (Oss, The Netherlands) are gratefully acknowledged for help with the injectability tests. Wouter Bult (Department of Nuclear Medicine, University Medical Center, Utrecht, The Netherlands) is gratefully acknowledged for assistance with the sieving procedure. This research was financially supported by SenterNovem (IS042016).

References

- [1] L. Jorgensen, E.H. Moeller, M. van de Weert, H.M. Nielsen, S. Frokjaer, Preparing and evaluating delivery systems for proteins, *European Journal of Pharmaceutical Sciences* 29 (2006) 174–182.
- [2] P. Bailon, W. Berthold, Polyethylene glycol-conjugated pharmaceutical proteins, *Pharmaceutical Science & Technology Today* 1 (1998) 352–356.
- [3] J. Panyam, V. Labhasetwar, Biodegradable nanoparticles for drug and gene delivery to cells and tissue, *Advanced Drug Delivery Reviews* 55 (2002) 329–347.
- [4] U. Bilati, E. Allmann, E. Doelker, Strategic approaches for overcoming peptide and protein instability within biodegradable nano- and microparticles, *European Journal of Pharmaceutics and Biopharmaceutics* 59 (2005) 375–388.
- [5] Y.-I. Chung, G. Tae, S.H. Yuk, A facile method to prepare heparin-functionalized nanoparticles for controlled release of growth factors, *Biomaterials* 27 (2006) 2621–2626.
- [6] J.A. Cadée, L.A. Brouwer, W. den Otter, W.E. Hennink, M.J.A. van Luyn, A comparative biocompatibility study of microspheres based on crosslinked dextran or poly(lactic-co-glycolic) acid after subcutaneous injection in rats, *Journal of Biomedical Materials Research* 56 (2001) 600–609.
- [7] V.R. Sinha, A. Trehan, Biodegradable microspheres for protein delivery, *Journal of Controlled Release* 90 (2003) 261–280.
- [8] W. Jiang, R.K. Gupta, M.C. Deshpande, S.P. Schwendeman, Biodegradable poly(lactic-co-glycolic acid) microparticles for injectable delivery of vaccine antigens, *Advanced Drug Delivery Reviews* 57 (2005) 391–410.
- [9] H.K. Kim, H.J. Chung, T.G. Park, Biodegradable polymeric microspheres with open/closed pores for sustained release of human growth hormone, *Journal of Controlled Release* 112 (2006) 167–174.
- [10] N.A. Peppas, P. Bures, W. Leobandung, H. Ichikawa, Hydrogels in pharmaceutical formulations, *European Journal of Pharmaceutics and Biopharmaceutics* 50 (2000) 27–46.
- [11] P. Gupta, K. Vermani, S. Garg, Hydrogels: from controlled release to pH-responsive drug delivery, *Drug Discovery Today* 7 (2002) 569–579.
- [12] N.A. Peppas, J.Z. Hilt, A. Khademhosseini, R. Langer, Hydrogels in biology and medicine: from molecular principles to biotechnology, *Advanced Materials* 18 (2006) 1345–1360.
- [13] W.E. Hennink, C.F. van Nostrum, Novel crosslinking methods to design hydrogels, *Advanced Drug Delivery Reviews* 54 (2002) 13–36.
- [14] V.V. Khutoryanskiy, Hydrogen-bonded interpolymer complexes as materials for pharmaceutical applications, *International Journal of Pharmaceutics* 334 (2007) 15–26.
- [15] A. Mahler, M. Rechtes, M. Rechter, S. Cohen, E. Gazit, Rigid, self-assembled hydrogel composed of a modified aromatic dipeptide, *Advanced Materials* 18 (2006) 1365–1370.
- [16] R.J.H. Stenekes, H. Talsma, W.E. Hennink, Formation of dextran hydrogels by crystallization, *Biomaterials* 22 (2001) 1891–1898.
- [17] E. Ruel-Gariepy, J.-C. Leroux, In situ-forming hydrogels – review of temperature-sensitive systems, *European Journal of Pharmaceutics and Biopharmaceutics* 58 (2004) 409–426.
- [18] S.R. Van Tomme, M.J. van Steenberghe, S.C. De Smedt, C.F. van Nostrum, W.E. Hennink, Self-gelling hydrogels based on oppositely charged dextran microspheres, *Biomaterials* 26 (2005) 2129–2135.
- [19] J. Berger, M. Reist, J.M. Mayer, O. Felt, N.A. Peppas, R. Gurny, Structure and interactions in covalently and ionically crosslinked chitosan hydrogels for biomedical applications, *European Journal of Pharmaceutics and Biopharmaceutics* 57 (2004) 19–34.
- [20] C.K. Kuo, P.X. Ma, Ionically crosslinked alginate hydrogels as scaffolds for tissue engineering: Part 1. Structure, gelation rate and mechanical properties, *Biomaterials* 22 (2001) 511–521.
- [21] C. Hiemstra, Z.Y. Zhong, S.R. Van Tomme, W.E. Hennink, P.J. Dijkstra, J. Feijen, Protein release from injectable stereocomplexed hydrogels based on PEG-PDLA and PEG-PLLA star block copolymers, *Journal of Controlled Release* 116 (2006) e19–e21.
- [22] S.J. De Jong, S.C. De Smedt, M.W.C. Wahls, J. Demeester, J.J. Kettenes-van den Bosch, W.E. Hennink, Novel self-assembled hydrogels by stereocomplex formation in aqueous solution of enantiomeric lactic acid oligomers grafted to dextran, *Macromolecules* 33 (2000) 3680–3686.

- [23] K.Y. Lee, D.J. Mooney, Hydrogels for tissue engineering, *Chemical Reviews* 101 (2001) 1869–1879.
- [24] J.L. Drury, D.J. Mooney, Hydrogels for tissue engineering: scaffold design variables and applications, *Biomaterials* 24 (2003) 4337–4351.
- [25] M.J. Mahoney, K.S. Anseth, Three-dimensional growth and function of neural tissue in degradable polyethylene glycol hydrogels, *Biomaterials* 27 (2006) 2265–2274.
- [26] S.G. Lévesque, M.S. Shoichet, Synthesis of cell-adhesive dextran hydrogels and macroporous scaffolds, *Biomaterials* 27 (2006) 5277–5285.
- [27] F. Brandl, F. Sommer, A. Goepferich, Rational design of hydrogels for tissue engineering: impact of physical factors on cell behavior, *Biomaterials* 28 (2007) 134–146.
- [28] S.P. Baldwin, W. Mark Saltzman, Materials for protein delivery in tissue engineering, *Advanced Drug Delivery Reviews* 33 (1998) 71–86.
- [29] S.R. Van Tomme, W.E. Hennink, Biodegradable dextran hydrogels for protein delivery applications, *Expert Review of Medical Devices* 4 (2007) 147–164.
- [30] S.R. Van Tomme, C.F. van Nostrum, S.C. De Smedt, W.E. Hennink, Degradation behavior of dextran hydrogels composed of positively and negatively charged microspheres, *Biomaterials* 27 (2006) 4141–4148.
- [31] W.N.E. van Dijk-Wolthuis, S.K.Y. Tsang, J.J. Kettenes-van den Bosch, W.E. Hennink, A new class of polymerizable dextrans with hydrolyzable groups: hydroxyethyl methacrylated dextran with and without oligolactate spacer, *Polymer* 38 (1997) 6235–6242.
- [32] R.J.H. Stenekes, O. Franssen, E.M.G. van Bommel, D.J.A. Crommelin, W.E. Hennink, The use of aqueous PEG/dextran phase separation for the preparation of dextran microspheres, *International Journal of Pharmaceutics* 183 (1999) 29–32.
- [33] O. Franssen, W.E. Hennink, A novel preparation method for polymeric microparticles without the use of organic solvents, *International Journal of Pharmaceutics* 168 (1998) 1–7.
- [34] E.J.W. Verwey, J.T.G. Overbeek, *Theory of the Stability of Lyotropic Colloids*, Elsevier, New York, 1948.
- [35] B.V. Derjaguin, L. Landau, Theory of the stability of strongly charged lyophobic sols and of the adhesion of strongly charged particles in solution of electrolytes, *Acta Physicochimica URSS* 14 (1941) 633–662.
- [36] R.J.H. Stenekes, S.C. De Smedt, J. Demeester, G. Sun, Z. Zhang, W.E. Hennink, Pore sizes in hydrated dextran microspheres, *Biomacromolecules* 1 (2000) 696–703.
- [37] D. Frenkel, B. Smit, *Understanding Molecular Simulation: From Algorithms to Applications*, second ed., Academic Press, London, 2002.
- [38] P. van de Wetering, N.J. Zuidam, M.J. van Steenberghe, O.A.G.J. van der Houwen, W.J.M. Underberg, W.E. Hennink, A mechanistic study of the hydrolytic stability of poly(2-(dimethylamino)ethyl methacrylate), *Macromolecules* 31 (1998) 8063–8068.
- [39] D.H. Grant, V.A. McPhee, Determination of methacrylic acid by coulometric titration, *Analytical Chemistry* 48 (1976) 1820.
- [40] Sterile single-use syringes, with or without needle, for insulin. ISO 8537 (E). 1991-05-01, 1991.
- [41] C.J. De Groot, M.J.A. Van Luyn, W.N.E. Van Dijk-Wolthuis, J.A. Cadee, J.A. Plantinga, W. Den Otter, W.E. Hennink, In vitro biocompatibility of biodegradable dextran-based hydrogels tested with human fibroblasts, *Biomaterials* 22 (2001) 1197–1203.
- [42] S.R. Van Tomme, B.G. De Geest, K. Braeckmans, S.C. De Smedt, F. Siepmann, J. Siepmann, C.F. van Nostrum, W.E. Hennink, Mobility of model proteins in hydrogels composed of oppositely charged dextran microspheres studied by protein release and fluorescence recovery after photobleaching, *Journal of Controlled Release* 110 (2005) 67–78.